

## Generation of photon number states

Edo Waks,<sup>1</sup> Eleni Diamanti,<sup>1</sup> and Yoshihisa Yamamoto<sup>1,2</sup>

<sup>1</sup>*Quantum Entanglement Project, ICORP, JST, E.L. Ginzton Laboratories, Stanford University, Stanford, CA 94305*

<sup>2</sup>*NTT basic research, Atsugi, Kanagawa, Japan*

(Dated: July 27, 2018)

The Visible Light Photon Counter (VLPC) has the capability to discriminate photon number states, in contrast to conventional photon counters which can only detect the presence or absence of photons. We use this capability, along with the process of parametric down-conversion, to generate photon number states. We experimentally demonstrate generation of states containing 1,2,3 and 4 photons with high fidelity. We then explore the effect the detection efficiency of the VLPC has on the generation rate and fidelity of the created states.

PACS numbers: 42.50.Ar,42.50Dv

Photon number states play an important role in quantum optics. Such states exhibit effects which contradict classical electromagnetic theory, such as anti-bunching and negativity of the Wigner function [1]. They also have important practical applications. In optical telecommunication, they achieve an optimal channel capacity [2, 3]. They can also improve the sensitivity of an interferometer to the Heisenberg limit [4]. In this limit, the minimum detectable phase shift is inversely proportional to the number of photons, rather than the square root of the number achieved by the standard quantum limit.

Recently, there has been tremendous effort in generating single photon states. This is often achieved by using single emitters such as molecules, quantum dots, or diamond color centers [5, 6, 7, 8, 9, 10, 11]. Although these sources hold great promise, they currently suffer from substantial collection losses. This creates a large vacuum contribution, which means that the generated state greatly deviates from one with exactly one photon. Furthermore, the extension of these devices to generating higher order photon number states remains a difficult problem. The generation of a two photon number state has been recently demonstrated in the microwave regime [12], using Rydberg atoms in a high-Q cavity. There have also been proposals for generation higher order optical photon number states using trapped atoms in an optical cavity [13]. The implementation of these schemes remains experimentally challenging.

There are generally two ways to engineer the quantum state of a system. The first is to start the system in a well known initial state, and turn on a unitary time evolution which transforms the initial state to the desired state. The second method is to make a non-destructive measurement of the quantum system, and project it onto the desired Hilbert space using the projection postulate of quantum mechanics. In this letter, we use the latter method of projection and conditional post-selection to generate a photon number state. This is done using the non-linear process of parametric down-conversion (PDC) in conjunction with a photon number detector known as the Visible Light Photon Counter (VLPC). In PDC, a

bright pump field is injected into a material which exhibits a second order non-linear dipole response. This non-linearity can cause a pump photon to spontaneously split into two photons of lower energy, referred to as the signal and idler. By appropriately adjusting the phase matching conditions of the process, the signal and idler can be made to propagate in different directions, allowing them to be spatially resolved. Since these two photons always come in pairs, if a signal photon is detected, there must be an idler photon in the conjugate mode. If a photon counter is placed in front of the signal arm and detects one photon, the corresponding idler arm is prepared in a state containing only one photon by the projection postulate of quantum mechanics. The photon counter in essence performs a non-destructive measurement of the idler arm.

The above scheme can be extended to generation of higher order number states. Suppose a short pump laser pulse is injected into a non-linear crystal. We can define the photon number operator  $\hat{n} = \int_T \hat{a}^\dagger(t) \hat{a}(t) dt$ , where the integral is taken over the pulse duration of the pump and  $\hat{a}(t)$  is the bosonic photon annihilation operator in the time domain. If  $n$  signal photons are detected by a photon counter in a given pulse, then the idler pulse is projected onto a state  $|\psi_i\rangle$  which satisfies the condition

$$\hat{n}|\psi_i\rangle = n|\psi_i\rangle. \quad (1)$$

That is, the idler mode is an eigenstate of the number operator with eigenvalue  $n$ . States which satisfy this special property are known as photon number states.

In order to implement the above scheme, the photon counter must be able to determine the exact number of photons in the signal arm within the short time duration of the pump pulse. Conventional photon counters such as avalanche photo-diodes (APDs) cannot do this, because they suffer from long dead time and large multiplication noise. Such detectors can only distinguish the zero photon case from the non-zero photon case in a pulse, making it impossible to generate photon number states.

Recently, a new type of photon counter known as the Visible Light Photon Counter (VLPC) [14], has

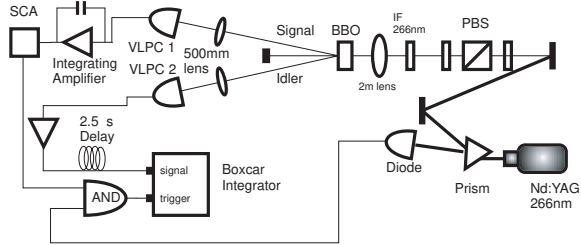


FIG. 1: Experimental setup for photon number generation.

been shown to have the capability to distinguish different photon number states with high quantum efficiency [15, 16, 17, 18]. When two photons are simultaneously detected by the VLPC, it generates an electrical pulse which is twice as large. This pattern holds for higher photon numbers. The pulse height can then be used to determine the number of detected photons.

The VLPC can do photon number detection due to two unique properties. First, the VLPC has an active area of 1mm in diameter. When one photon is detected, it forms a  $5\mu\text{m}$  diameter dead spot on the detector surface, leaving the rest of the active area available for subsequent detection events. As long as the probability that two photons land on the same spot is small, which is true if the incident light is not too tightly focussed, all of the photons will be detected. This circumvents the dead time problem which conventional APDs suffer from. Second, the VLPC has extremely low multiplication noise. Multiplication noise refers to the fluctuations in the number of electrons emitted by a detector in response to a photodetection event. These fluctuations limit the ability of the detector to infer photon number [18]. Multiplication noise is quantified by a parameter known as the Excess Noise Factor  $F = \langle M^2 \rangle / \langle M \rangle^2$ , where  $M$  is the number of electrons emitted by the detector due to a photon detection. In the ideal limit where  $F = 1$ , the detector emits a deterministic number of electrons for each detection. APDs with single carrier multiplication, which achieves the best noise performance, still have a large excess noise factor of  $F = 2$  [19], making it impossible to discriminate photon numbers. The VLPC, in contrast, achieves nearly noise free multiplication with  $F = 1.03$  [18, 20].

The experimental setup for generating photon number states is shown in Figure 1. A 266nm pump source is generated from the fourth harmonic of a Q-switched Nd:YAG laser. The pump pulses have a duration of 20ns, and a repetition rate of 45kHz. A dispersion prism separates the fourth harmonic from the residual second harmonic, which is used to illuminate a high speed photodiode to generate a triggering signal. The fourth harmonic pumps a BBO crystal, which is set for non-collinear degenerate phase-matching. In this condition, the signal and idler waves are both 532nm in wavelength and have a divergence angle of 1 degree from the pump. The pump

is loosely focused before the BBO crystal to achieve a minimum waste at the collection lens. This results in a sharper two-photon image which enhances the collection efficiency [21].

Two VLPC detectors are used in this experiment. Each detector is held in a separate helium bath cryostat and cooled down to 6-7K, which is the optimum operating temperature. The VLPC is sensitive to photons with wavelengths of up to  $30\mu\text{m}$ , so it must be shielded from room temperature thermal radiation. This is achieved by encasing the detector in a copper shield, which is cooled down to 6K. Acrylic windows at the front of the copper shield are used as infra red filters. These windows are highly transparent at visible wavelengths and simultaneously nearly opaque at 2-30 $\mu\text{m}$  wavelengths.

VLPC 1 is used as the triggering detector which detects the number of photons generated in the signal arm on a given laser pulse. The output of VLPC 1 is amplified by an integrating amplifier, which generates an electrical pulse whose height is proportional to the number of emitted electrons. The height of the pulse is discriminated by a single channel analyzer (SCA). A logical AND is performed between the output of the SCA and the output of the photodiode to reject all detection events which occur outside of the pulse duration. Figure 2a shows a pulse height histogram of VLPC 1. This histogram features a series of peaks corresponding to different photon number states. The SCA can select pulse heights corresponding to one, two, three, and four photon events. The decision window set by the SCA for each photon number event is shown by the shaded areas in the figure.

VLPC 2 is placed in the idler arm, and used to verify that the correct photon number state was generated. The output of VLPC 2 is amplified, and connected to the signal input of a boxcar integrator. On each pulse from the SCA, the output of VLPC 2 is integrated over a  $2\mu\text{s}$  window, which is sufficiently large to encompass the entire electrical pulse (determined by the bandwidth of subsequent amplifiers). Figure 2b shows a pulse area distribution of VLPC 2 with no post-selection from VLPC 1, at a pump excitation power of  $40\mu\text{W}$ . This distribution also features a series of peaks corresponding to the different photon numbers, starting with the first peak which is a zero photon event. In order to calculate the photon number distribution, each peak is fit to a gaussian. The area of each gaussian is normalized by the total area of all the peaks. The calculated photon number distribution is shown in the inset.

Both VLPCs have imperfect detection efficiencies due to internal detection losses of the VLPC itself, as well as external losses from the collection optics. The efficiency is measured by comparing the coincidence rate between the two detectors to the singles count rates. From this measurement we determine the detection efficiency of VLPC 1 to be 0.68, and VLPC 2 to be 0.58.

The detection efficiency of the monitoring detector

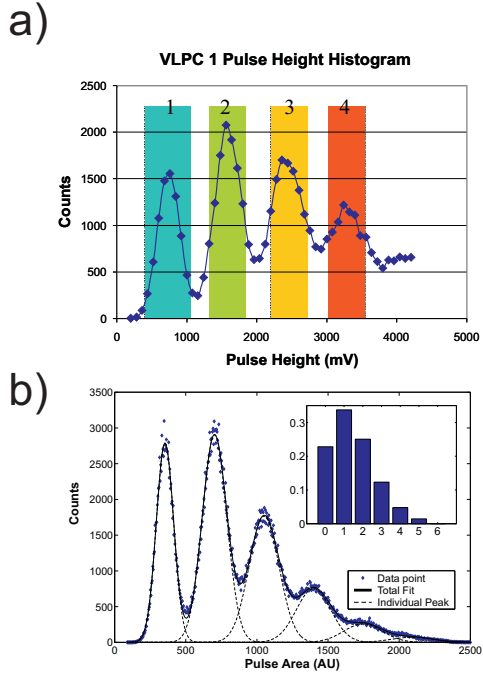


FIG. 2: Photon number detection from the VLPCs. **a**, pulse height histogram from VLPC 1 after an integrating amplifier. The histogram features a series of peaks corresponding to the photon number distribution of the parametric down-conversion output. An SCA is used four different regions, corresponding to the different photon number events, shown by the shaded regions. **b**, a pulse area histogram of VLPC 2 when no post-selection is done from VLPC 1. Each peak is fit to a gaussian to calculate the photon number distribution, shown in the inset.

(VLPC 2) can be corrected for, because we are interested mainly in how many photons were actually present in the idler arm, not how many have been detected. To do this, we can define  $p_j$  as the probability that  $j$  photons were generated in the idler pulse, and  $f_i$  as the probability that  $i$  photons were detected. These two probabilities are related by the linear loss model  $f_i = \sum_{j=i}^{\infty} \binom{j}{i} \eta^i (1-\eta)^{j-i} p_i$ . The above transformation needs to be inverted. In order to do this we truncate the photon number distribution at some number  $n$ , which is sufficiently large so that  $p(n+1) \approx 0$  is a good approximation. The initial and final probability distributions are then related by a constant matrix, which can simply be inverted. This matrix can also be modified to account for dark counts in a straightforward way.

The detection efficiency of the triggering detector (VLPC 1) plays a more subtle role in the experiment. Detection losses can result in a higher order photon number state being misinterpreted by the detector as the correct photon number. Because of this, the probability distribution in the idler arm will no longer be an exact photon number, but a mixture of the desired number plus higher order number states. This results in a degradation of the

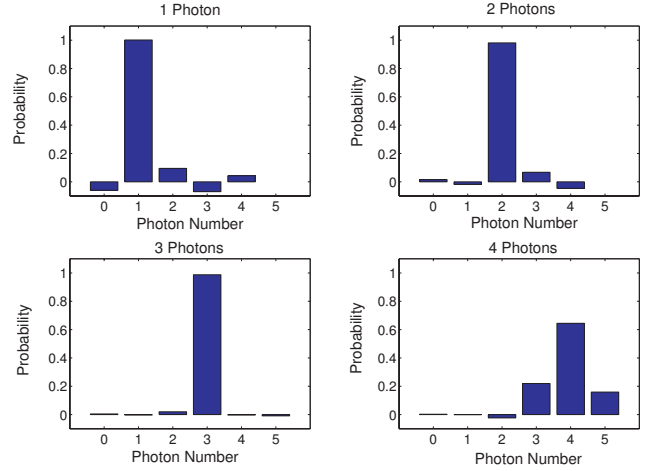


FIG. 3: Results of the photon number generation experiment. The photon number distributions, after correcting for detection efficiency and dark counts of VLPC 2, are plotted for the reported number  $n=1,2,3$ , and 4 by VLPC 1. The detection efficiency and dark counts of VLPC 2 are measured independently.

fidelity, defined as the overlap between the desired state and the actual generated state. For a state containing  $n$  photons the fidelity is simply the probability that  $n$  photons are generated.

When the pumping intensity is low, the efficiency of the triggering detector does not play a major role. If the triggering detector sees  $n$  photons, it is true with very high probability that the same number of photons are present in both arms. The probability that there were more photons present is extremely low, because low pumping intensity makes the probability of generating higher order photon pairs negligible. Figure 3 shows the experimental results at this low pumping intensity regime. The figure shows the photon number distributions measured by VLPC 2, after correcting for detection efficiency and dark counts, when VLPC 1 post-selects a one, two, three, and four photon event. For one, two, and three photon post-selection, a nearly ideal photon number state is generated. For four photon post-selection however, there are contributions from three and five photon number states. These contributions are attributed to the smearing between the four photon peak and its next nearest neighbors in the pulse height histogram of VLPC 1 (Fig. 2a). The smearing is caused by buildup of multiplication noise, which puts a limit on the photon number resolution at higher numbers [18]. Note that, in a few cases, the corrected probability distribution becomes negative. This erroneous effect is caused by numerical errors in the probability reconstruction.

As we increase the pumping power, the imperfect detection efficiency of VLPC 1 will result in degraded fidelity, as was previously discussed. On the other hand, higher pump powers will increase the probability that the

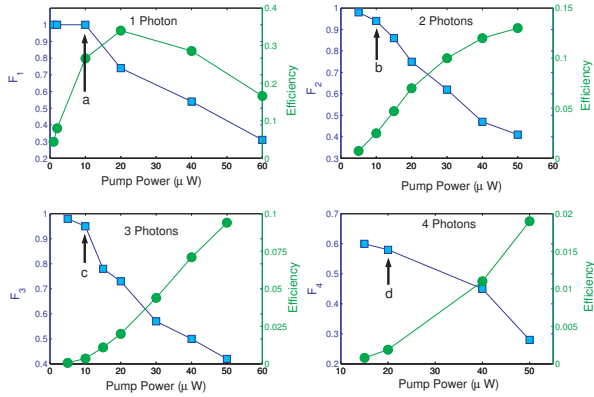


FIG. 4: The generation rate (circles) and fidelity (squares) are plotted as a function of pump power. The fidelity corresponds to the left y-axis, while the generation efficiency corresponds to the right y-axis.

correct number of photons were generated, and hence the generation rate of the desired photon number state. This leads to a natural tradeoff between the state fidelity and generation rate of photon number states. The extent of the tradeoff is determined mainly by the detection efficiency of VLPC 1. In order to determine this tradeoff, we measure the fidelity and generation rate as a function of pump power for the four different photon number states. The results are shown in Figure 4. For all four cases, increasing the pump power results in higher generation rates but decreased fidelity. In the figure, four data points are labelled as a, b, c, and d. These points designate the pumping intensity before the fidelity begins to drop for one, two, three, and four photon number states. The generation rate and fidelity at these four points are: a - 11800 Hz and  $F_1=1.0$ , b - 1100 Hz and  $F_2=0.94$ , c - 160 Hz and  $F_3=0.95$ , d - 84 Hz and  $F_4=0.6$ . The above generation rates are already large enough to be useful for practical experiments. These rates are achieved using only a 45kHz pump repetition rate. The rates could be significantly enhanced by simply using a pump laser with a faster repetition rate.

We conclude by discussing some of the future extensions of this work. There are two main drawbacks to the experimental scheme we present in this letter. First, the setup does not allow for generation of photon number states on demand. The time in which the number state is generated is known but uncontrollable. This problem can be solved in principle by setting up a large parallel array of photon number generators along with an optical switch. By making the array large, the probability that at least one of the number state generators will generate the right photon number can be made arbitrarily close to unity. Of course, with the current setup such a solution is impractical, but perhaps the engineering of VLPC arrays, along with more compact two photon sources based on waveguide technology, may make such a solution pos-

sible.

The second drawback of our experiment is that the pump pulse to the down-conversion crystal has a 20ns duration, as opposed to the coherence time of the down-converted photons which is on the order of femtoseconds. This means that, although the states we generate are eigenfunctions of the photon number operator, the quantum mechanical wavefunctions of the photons is not fixed. In fact the wavefunction of each photon will generally fluctuate from shot to shot. A more ideal source would generate a state in which both the number and wavefunction of the photons is constant. The best case scenario would be the generation of a so-called n-photon Fock state, which is a state containing n-photons with identical wavefunctions. Our setup could be extended to generate such a state by replacing the pumping laser with a femtosecond pulse laser, so that the pulse duration is on the order of the coherence length of the photons. This could open up the door for interesting new experiments in quantum information using photon number states.

---

- [1] D. Walls and G. Milburn, *Quantum optics* (Springer, New York, 1995).
- [2] Y. Yamamoto and H. Haus, Rev. Mod. Phys. **54**, 1001 (1986).
- [3] C. Caves and P. Drummond, Rev. Mod. Phys. **66**, 481 (1994).
- [4] M. Holland and K. Burnett, Phys. Rev. Lett. **86**, 1502 (2001).
- [5] C. Santori et al., Phys. Rev. Lett. **86**, 1502 (2001).
- [6] J. Kim, O. Benson, H. Kan, and Y. Yamamoto, Nature **397**, 500 (1999).
- [7] B. Lounis and W. Moerner, Nature **407**, 491 (2000).
- [8] P. Michler et al., Science **290**, 2282 (2000).
- [9] E. Moreau et al., App. Phy. Lett. **79**, 2865 (2001).
- [10] A. Beveratos et al., Euro. Phys. J **18**, 191 (2002).
- [11] Z. Yuan et al., Science **295**, 102 (2002).
- [12] B. Varcoe et al., Nature **403**, 743 (2001).
- [13] K. Brown et al., Phys. Rev. A **67**, 043818 (2003).
- [14] G. Turner et al., *Visible light photon counters for scintillating fiber applications: I. characteristics and performance*, Proceedings of the Workshop on Scintillating Fiber Detectors (1993), pg. 613.
- [15] S. Takeuchi, J. Kim, and Y. Yamamoto, App. Phys. Lett. **74**, 1063 (1999).
- [16] M. Atac et al., Nucl. Instrum. & Methods in Phs. Research A **314**, 56 (1994).
- [17] J. Kim, S. Takeuchi, and Y. Yamamoto, App. Phys. Lett. **74**, 902 (1999).
- [18] E. Waks et al., quant-ph/0308054.
- [19] R. McIntyre, IEEE Trans. Electron Devices **ED-13**, 164 (1966).
- [20] J. Kim, Y. Yamamoto, and H. Hogue, App. Phys. Lett. **70**, 2852 (1997).
- [21] C. Monken, P. S. Ribeiro, and S. Padua, Phys. Rev. A **57**, R2267 (1998).